Transequatorial Flow of Antarctic Bottom Water in the Western Atlantic Ocean: Abyssal Geostrophy at the Equator*

M. S. McCARTNEY AND R. A. CURRY

Woods Hole Oceanographic Institution, Woods Hole, Massachusetts

30 January 1992 and 10 September 1992

ABSTRACT

In its general northward flow along the western trough of the Atlantic, Antarctic Bottom Water (AABW) must pass over several sills separating the various abyssal basins. At the equator, the western trough is deformed by major east–west offsets of the Mid-Atlantic Ridge and the continental margin of Brazil, forming a nearly zonal abyssal channel about 250 km wide, centered at the equator, and extending approximately 1000 km along its axis, in which the AABW is confined. Thus, the general northward flow of AABW is topographically constrained to be westward as it crosses the equator. A hydrographic section across this channel at 37°W shows the AABW isopycnals to be "bowl" shaped within and beneath the level of the channel walls. The equatorial geostrophic relation permits us to compute a zonal velocity from the well-defined parabolic distribution of dynamic height, relative to a reference level at the transition between AABW and the overlying deep water. Here 4.3×10^6 $m^3 s^{-1}$ is estimated for the westward—and ultimately northward—transport of AABW. Although this value exceeds previous estimates of net northward transport in the Brazil and Guiana basins made from International Geophysical Year data of the late 1950s, it fits well into an overall scenario constructed from transport estimates made from section data collected during the 1980s. This scenario includes a flow of approximately 7×10^6 $m^3 s^{-1}$ of AABW into the Brazil Basin from the south. The magnitude of the northward flow diminishes as it moves toward the equator indicated by estimates of 6.7×10^6 $m^3 s^{-1}$ at 23°S and 5.5×10^6 $m^3 s^{-1}$ at 11°S. At the equator, 4.3×10^6 $m^3 s^{-1}$ exits the Brazil Basin to continue northward across the Guiana Basin, and an unquantified amount flows through the Romanche Fracture Zone into the eastern basin. The northward decrease in AABW suggests an upwelling across isotherms. The difference in transports between 11°S and the equator, 1.2×10^6 $m^3 s^{-1}$, is an estimate of the combined amounts of AABW being upwelled and exiting the basin through the Romanche Fracture Zone. In the Guiana Basin at 4°N, AABW transport is estimated at 4.0×10^6 $m^3 s^{-1}$. This flow subsequently splits into two approximately equal flows: continued northward flow through the Guiana Basin, and eastward flow through the Vema Fracture Zone at 11°N to the eastern basin.

1. Introduction

The abyss of the Atlantic Ocean is divided into two north–south trending troughs by the Mid-Atlantic Ridge. Cold dense waters enter the western trough from sources in the polar and subpolar seas of both hemispheres and flow toward the opposite hemisphere as deep western boundary currents (DWBC). The northern source waters and their progressively altered forms to the south are collectively and loosely defined as the North Atlantic Deep Water (NADW). The southern source waters and their progressively altered forms are likewise referred to as the Antarctic Bottom Water (AABW). Progressive alteration reflects the entrainment/detrainment of heat, salt, mass, and other physical and chemical properties along the path of the flow. Mixing between the vertically superimposed NADW and AABW contributes greatly to their alteration. Where the influence of southern source waters can be recognized, the AABW is, in general, locally more dense, situated between the NADW and the seafloor. As a result, the topography of abyssal basins and interconnecting passages strongly influences the lateral distribution of AABW properties.

Estimates of the AABW net transport have been made from various sections crossing the western and eastern troughs. Because conventional geostrophic estimates cannot be made directly at the equator, the transequatorial transport of AABW has only been inferred in the western trough from sections located several degrees to the north. This paper takes advantage of a topographic peculiarity in the equatorial zone of the western trough to make a direct geostrophic estimate of the transequatorial exchange of AABW using a section that crosses the equator near the western boundary. Abyssal ridges, zonally oriented north and south of the equator, constrain the AABW to flow westward along the equator as it crosses from the Southern Hemisphere to the Northern Hemisphere. A meridional hydrographic section across this east–west

* Contribution Number 7973 from the Woods Hole Oceanographic Institution.

Corresponding author address: Dr. Michael S. McCartney, Woods Hole Oceanographic Institution, Woods Hole, MA 02543-1047.

channel reveals parabolic isopycnals centered on the equator in the AABW. By assuming a predominantly zonal flow in the channel, the equatorial geostrophic expression for the zonal flow produces a velocity profile and a transport estimate of 4.3×10^6 m^3 s^{-1}.

The structure of the remainder of this paper is as follows. Section 2 discusses the general distribution of the AABW in the Atlantic Ocean. Section 3 describes the basic property fields of the 1983 CTD section crossing the equatorial channel, the selection of a reference level, and the application of equatorial geostrophy to produce an estimate of the transequatorial transport of AABW at the equator. In section 4, we present an overall picture of AABW transport through the western Atlantic.

2. Background

The global distribution of bottom water characteristics has been charted and discussed by Mantyla and Reid (1983), and here we briefly review their chart of bottom potential temperature, θ_B, in the Atlantic Ocean (Fig. 1). A gradual northward increase in θ_B values characterizes each of the major abyssal basins in the western trough, while steeper θ_B gradients are delineated in the constricted passages and silled channels connecting these basins.

From the Weddell Sea, typified by θ_B values between $-0.9°$ and $-0.8°$C, to the Argentine Basin, where values range between $-0.3°$ and $-0.2°$C, a 0.5°C rise occurs in θ_B. Tongue-shaped isotherms, for example, $\theta_B = -0.5°$C, trace the flow of AABW through the South Sandwich Trench and the Georgia Basin, under the Antarctic Circumpolar Current, and into the southern Argentine Basin. Whitworth et al. (1991) have published current meter measurements of this flow into the Argentine Basin, reporting a DWBC transport of 8.2×10^6 m^3 s^{-1} for AABW colder than 0.2°C.[1] Water warmer than this temperature cannot be differentiated from water entering the basin through the Drake Passage. The relation of this DWBC transport to the net meridional transport of AABW in the Argentine Basin, however, remains unclear. Although it exceeds Wright's (1970) geostrophic estimate of 5.2×10^6 m^3 s^{-1} at the International Geophysical Year (IGY) 32°S section, the lower estimate may reflect poor positioning of stations at the western boundary.

From the Argentine Basin, AABW transits the Rio Grande Rise (near 32°S, Fig. 2a) through the Vema and Hunter channels and flows into the Brazil Basin where θ_B values rise slightly to between 0.0° and 0.3°C. Hogg et al. (1982) reported a transport of 4.1×10^6 m^3 s^{-1} through the Vema Channel for AABW colder than 1.58°C. The net northward flow into the Brazil Basin is believed to be larger than this due to additional

FIG. 1. The distribution of near bottom potential temperature in the Atlantic Ocean (from Mantyla and Reid 1983).

flows along the continental slope west of the Vema Channel and through the Hunter Channel. AABW exits the Brazil Basin at its northern boundary via two routes: part is diverted to the eastern trough through the Romanche Fracture Zone at the equator, while the remainder crosses the equator into the western trough of the North Atlantic.

Proceeding northward in the western trough, AABW enters the North Atlantic Basin, which is dominated by the Nares Abyssal Plain and is separated from the Brazil Basin by a series of abyssal plains collectively called the Guiana Basin. Between the equator and 18°N, AABW flows through the narrowed western trough passing successively over the Ceara, Para, Demerara, and Barracuda Abyssal plains. The Ceara Abyssal Plain is, in actuality, a regional topographic rise, shoaling to a sill depth < 4500 m near 3°N, compared to depths > 5500 m in the northern Brazil and northern Guiana basins. Whitehead and Worthington (1982) estimated the transport of AABW colder than 1.9°C at 4°N (between the Ceara and Para Abyssal plains) to be 0.8 or 2.0 ($\times 10^6$ m^3 s^{-1}); McCartney (1993a) disputes these estimates and claims 4.0×10^6 m^3 s^{-1} at this location. About one-half of this flow is diverted into the eastern trough through the Vema Fracture Zone at 11°N (McCartney et al. 1991). The remainder spreads northward in the western trough,

[1] All temperatures referred to in this paper are potential temperatures.

fading in intensity, but is recognizable as θ_B values near 1.7°C northeast of Bermuda (Sohm Abyssal Plain) and near 1.8°C in the Newfoundland Basin [distinguishable from northern source waters by its higher silicate; McCartney (1992)].

The largest increase in θ_B between adjacent basins (1°C) occurs across the equator. The mechanism for this warming is the topographic restriction of colder water from northward flow in at least one, possibly two, locations (Fig. 2). The first is a topographic sill located at the entrance to the equatorial channel in the northwest corner of the Brazil Basin. Formed by the eastward broadening of the continental slope and the westward extension of the Mid-Atlantic Ridge, it prevents water deeper than 4500 m—and colder than 0.6°C—from entering the Guiana Basin. A second barrier, although not sharply defined, is formed by the Ceara Abyssal Plain, which gradually shoals to a depth of less than 4500 m between 1°N and 4°N. Near this rise, θ_B is about 1.0°C (Whitehead and Worthington 1982), compared to 0.6°C in the equatorial channel and 1.2°C in the northern Guiana Basin (Demerara Abyssal Plain, depths > 5500 m). Whitehead and Worthington (1982) described this still as a barrier preventing the deeper (and colder) AABW from further northward flow while permitting only AABW warmer than 1°C to spill over the sill and continue its northward flow.

This paper focuses on the equatorial zone through which the AABW transits from the Brazil Basin into the Guiana Basin and makes some estimates of the magnitude of the northward AABW transport. Although the ability to use geostrophic methods to compute meridional transport normally breaks down at the equator, the topography in this particular region—detailed in Fig. 2b—presents us with a special case. The north–south trending Mid-Atlantic Ridge yields to a series of westward offsets between 5°S and 15°N that incline the ridge axis to trend NW–SE, paralleling the South American coastline. At the equator, fracture zones and other tectonic features combine to create topography with a nearly east–west trend: the Parnaiba Ridge projects eastwards from the continental slope of Brazil towards the Pernambuco Abyssal Plain near 2°S, while another narrow ridge projects westward from the midocean ridge onto the southern Ceara Abyssal Plain near 1°N. The latter ridge originates in the neighborhood of the St. Peter and St. Paul Rocks and forms the north wall of the St. Paul Fracture Zone. Neither of these ridges completely blocks the western trough, but they do overlap for the longitude range between 35° and 40°W. The result is a zonal channel at the equator, open to the northwest at 40°W and open to the southeast at 35°W. The overall northward flow of AABW is thus topographically constrained to approach the equator from east of 35°W, turn westward and flow along the equator between 2°S and 1°N, finally turning northward as it exits the channel west of 40°W. The crest height of the north wall represents the vertical limit for this topographic constraint. Our potential temperature section indicates all water colder than 2.0°C lies beneath this crest height; however, breaks or gaps in this wall could conceivably permit AABW to leak across the equator unconstrained by this channel.

A section of CTD stations with supportive water sample work was made in 1983 across this equatorial channel (locations on Fig. 2). This report uses that section to estimate the westward transport of AABW geostrophically, implementing the latitudinally differentiated form of the more familiar midlatitude geostrophic balance. This equatorial geostrophic formulation relates the product of the planetary β and the zonal flow speed to the latitudinal curvature of the dynamic height field. It is the channeling of the AABW to westward flow along the equator for a limited longitudinal range—and an element of luck—that permits this application of the equatorial geostrophic relation. The luck factor involves the situation of the abyssal current almost directly on the equator at the time of the CTD work: the dynamic height field is of nearly perfect parabolic form with zero slope at the equator. The serendipitous nature of a single section yielding such symmetry is evidenced by two points. First, the symmetry in the dynamic height field deteriorates significantly above the AABW; it is common in thermocline applications of the equatorial geostrophic formulation to have to average together several sections to achieve a field symmetric about the equator. Second, a subsequent reoccupation of this section in 1989 showed an AABW dynamic height decidedly asymmetric about the equator.

3. Antarctic Bottom Water at the equator and an estimate of its transequatorial transport

In the summer of 1983, the R/V *Knorr* occupied a long section of CTD stations near 35°W between Greenland and Brazil. After some focused work on the deep and bottom water flow at the Vema Fracture Zone (McCartney et al. 1991), the section crossed the Mid-Atlantic Ridge extending southward across the western trough of the Atlantic to Capo de Sao Roque, the northeast extremity of the South American continent. The equatorial channel was crossed near 36°45′W and included stations at latitudes ±1.25°, ±0.75°, ±0.33°, and 0.0°. The data collected included CTD profiles of temperature, salinity, and oxygen, and up to 24 water samples per station. The water samples were processed for salinity and oxygen content, for calibration of the CTD instrument, and for the three nutrients, silica, nitrate, and phosphate. In April 1989, after completing a transect of the South Atlantic near 25°W, a partial repeat of the section across the equatorial channel was obtained from the R/V *Melville,* with a similar suite of measurements. Territorial water technicalities

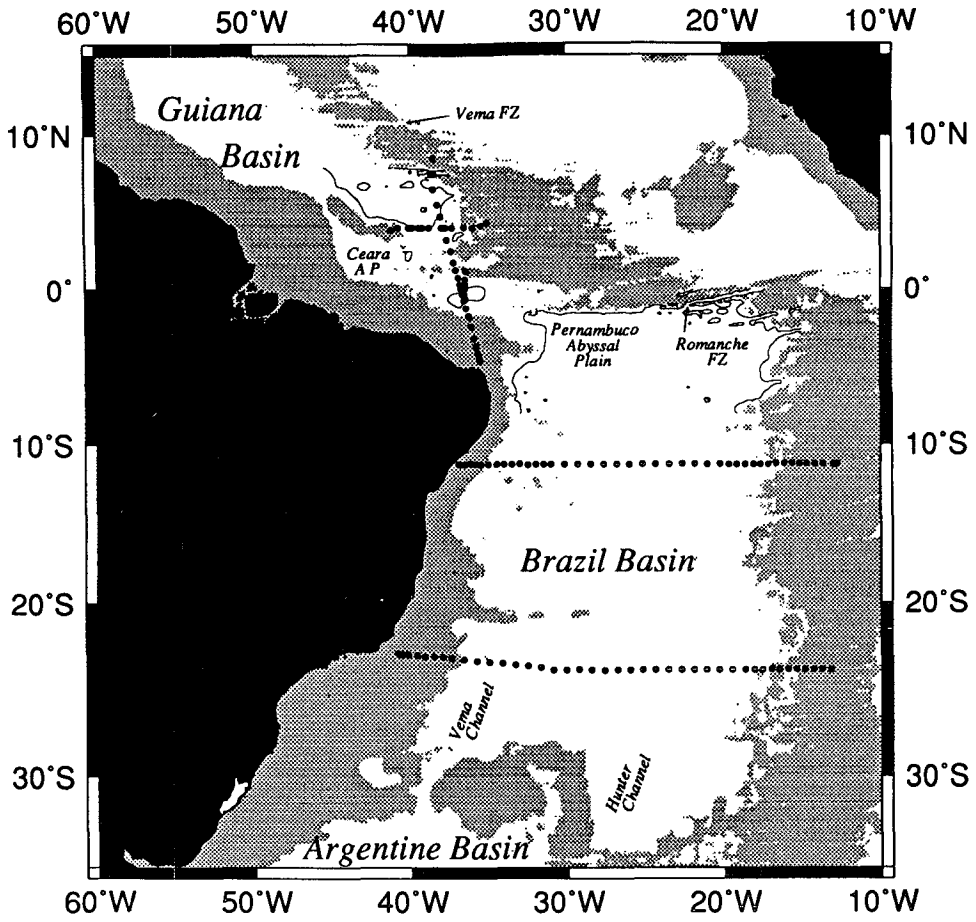

FIG. 2a. Locations of the primary transequatorial R/V *Knorr* section from 1983 and the 1989 R/V *Melville* repeat occupation at the equator, both used in Figs. 3 and 4. Sections near 11°S and 23°S, from R/V *Oceanus* in 1983, are shown in Fig. 5; and the *Oceanus* stations near 4°N collected in 1977 are the focus of studies by Whitehead and Worthington (1982) and McCartney (1993a). Shading indicates depths shallower than 4000 m, and the 4500-m contour is included in the tropics to delineate the equatorial sill [bathymetry from the "Etopo5" database, National Geophysical Data Center (1988)].

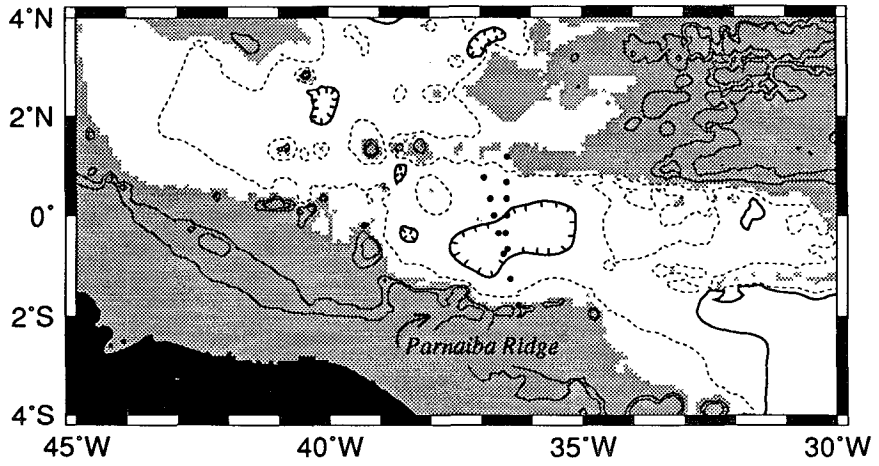

FIG. 2b. An expanded view of the equatorial zone, as in (a). Depths shallower than 4000 are shaded, with 3000- and 3500-m contours within the shading. The clear area includes the 4250- (dashed) and 4500-m (solid) contours.

moved the location of this section slightly east of the original to 36.5°W and limited its extent from 0.66°S to 1.17°N. The property fields for this repeat section are included as panels with the primary section figures.

Figure 3 depicts the fields of potential temperature, potential density, and salinity. The θ_B values are uniformly 0.62°C in the equatorial channel, accounting for about one-half the transequatorial warming of bottom temperatures between 0.19°C of the northern Brazil Basin to 0.98°C at the Ceara Abyssal Plain sill. No significant change in near-bottom temperature was observed in the two occupations of this site. Comparably situated stations from both sections yield averaged θ_B values of 0.626°C (1983) and 0.628°C (1989). Bottom temperatures at the equator were recorded as 0.617°C and 0.612°C, respectively. The AABW is characterized by a relatively homogenous layer, 0.62°–1.2°C and 100–200 m thick, overlain by a layer of steeper gradients where temperatures range from 1.2° to 1.9°C.

Structure in the temperature and density fields indicates a degree of dynamical activity, which is surprising for this latitude. The isopleths oscillate 100–200 m over horizontal distances of 100–300 km, which converts to significant geostrophic shear given the diminuitive nature of the Coriolis parameter. Because significant geostrophic shear emerges only where isopycnal slopes are coherent over a considerable depth range

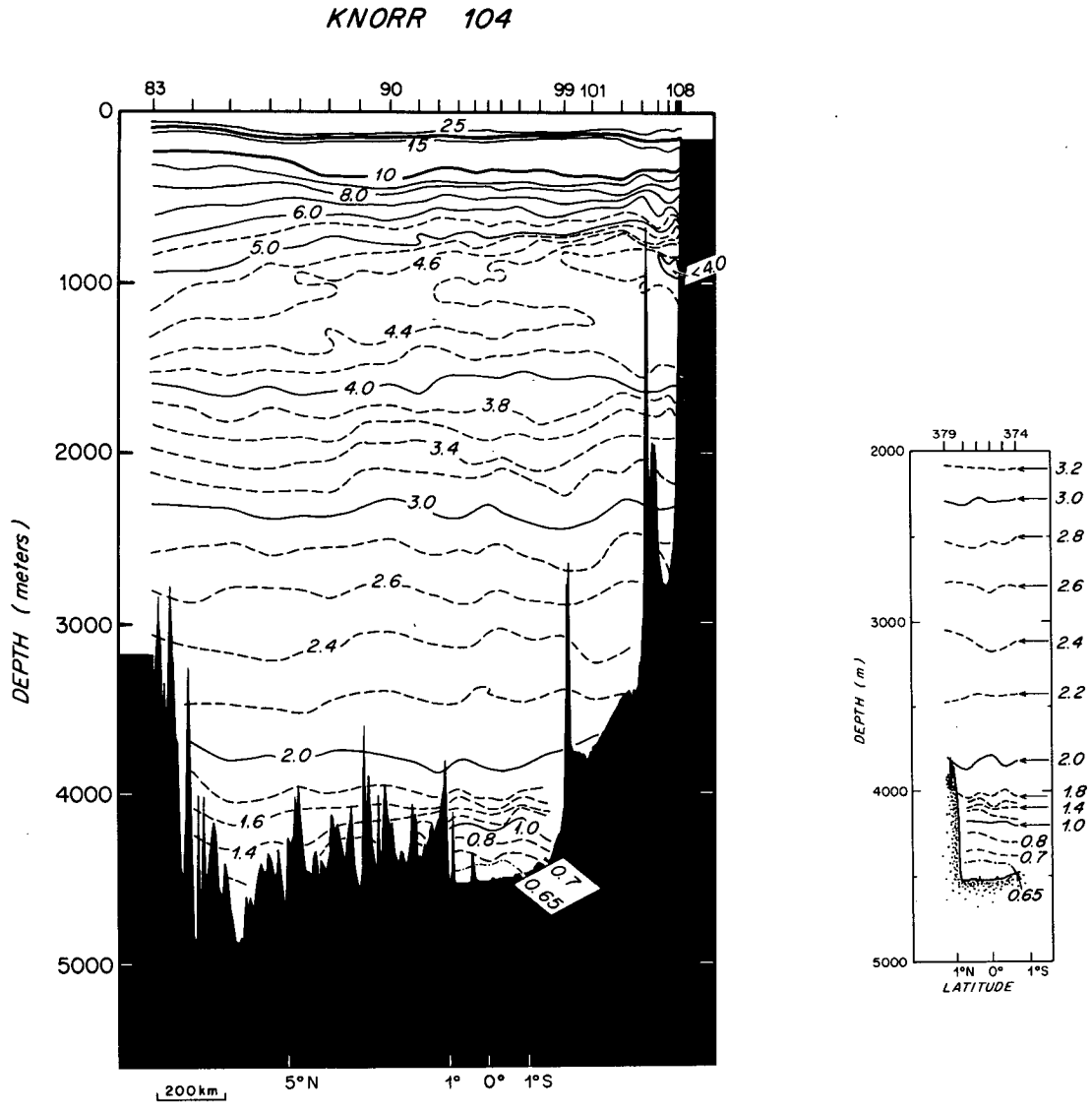

FIG. 3. Property distributions along a quasimeridional section near 37°W (position shown in Fig. 2a) made from the R/V *Knorr* in August 1983. The smaller panels show the partial reoccupation from R/V *Melville* in April 1989. (a) Potential temperature (°C).

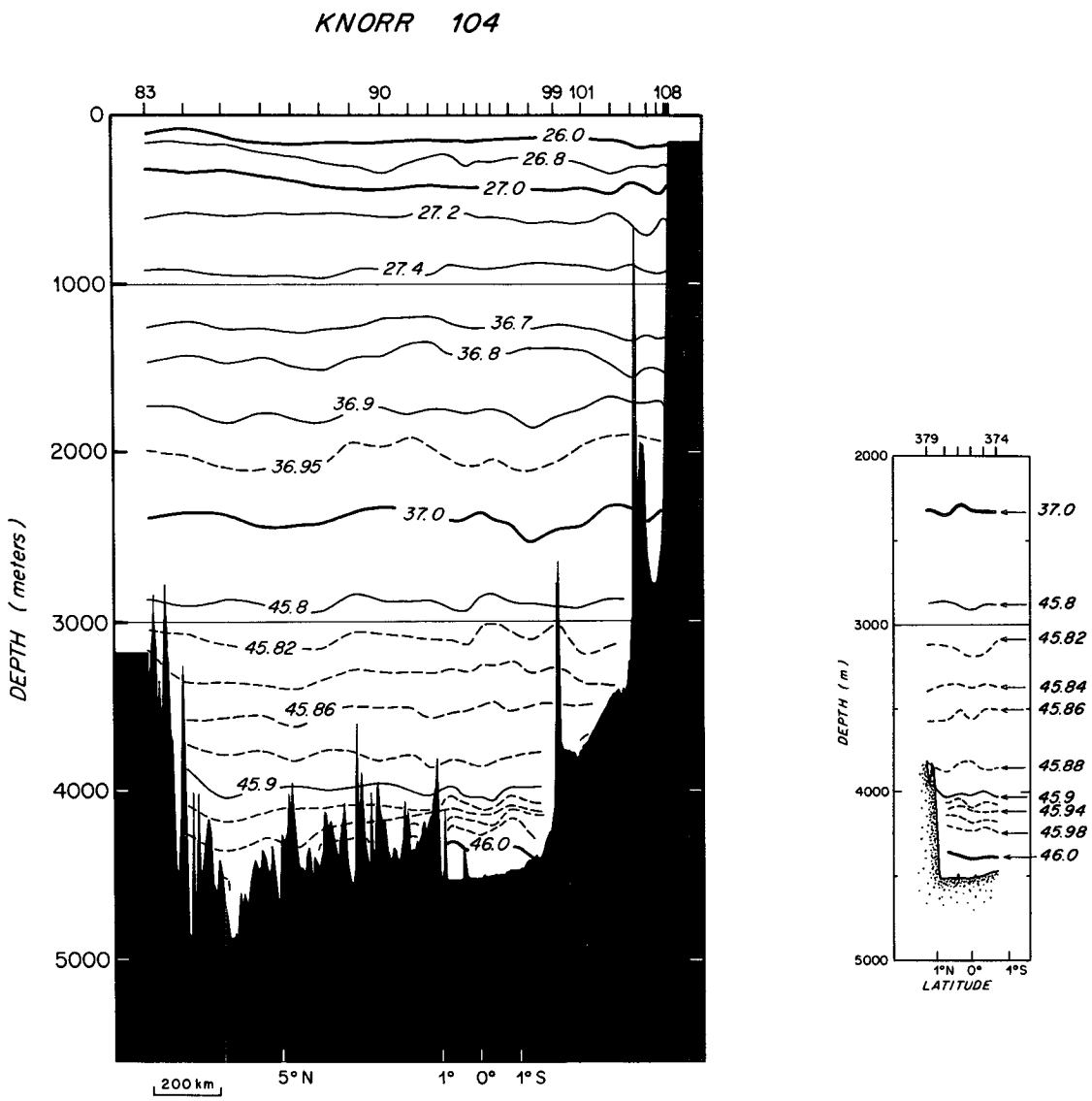

FIG. 3. (*Continued*) (b) Potential density anomaly (EOS80, g kg^{-1}).

(or where the vertical density gradient is steep), the actual shear is considerably less than the temperature and density fields suggest. We do note, however, several small shear reversals within a few hundred kilometers of the equator. Possibly these represent the edges of deep equatorial jets characterized by high vertical mode number on which Ponte et al. (1990) reported. The water mass layering visible in the NADW within the channel (Fig. 3) also suggests high vertical mode number.

Although the 1989 CTD survey did not fully cross the equatorial channel, the partial section depicts a significant deviation from the symmetry of the 1983 section. Because its abyssal dynamic height field is sloped at the equator, the special form of the geostrophic equation cannot be applied to this section by itself. It appears that this is the more usual case in oceanography: other investigators implementing this method in the upper ocean report it is often necessary to average several profiles in order to obtain a symmetry suitable for use in this equatorial geostrophic computation (cf. Moum et al. 1987). We consider the 1983 section a fortuitous occurrence indeed, presenting us with an opportunity to estimate transport from a synoptic, rather than averaged, set of data.

We will make use of the equatorial geostrophic relation that has seen much application in the upper water column the last few years (e.g., Hayes 1982; Lukas and Firing 1984; Moum et al. 1987). The conventional midlatitude geostrophic relation is derived from the equations of motion under the assumptions of steadiness, linearity, negligible stress, and hydrostatic balance.

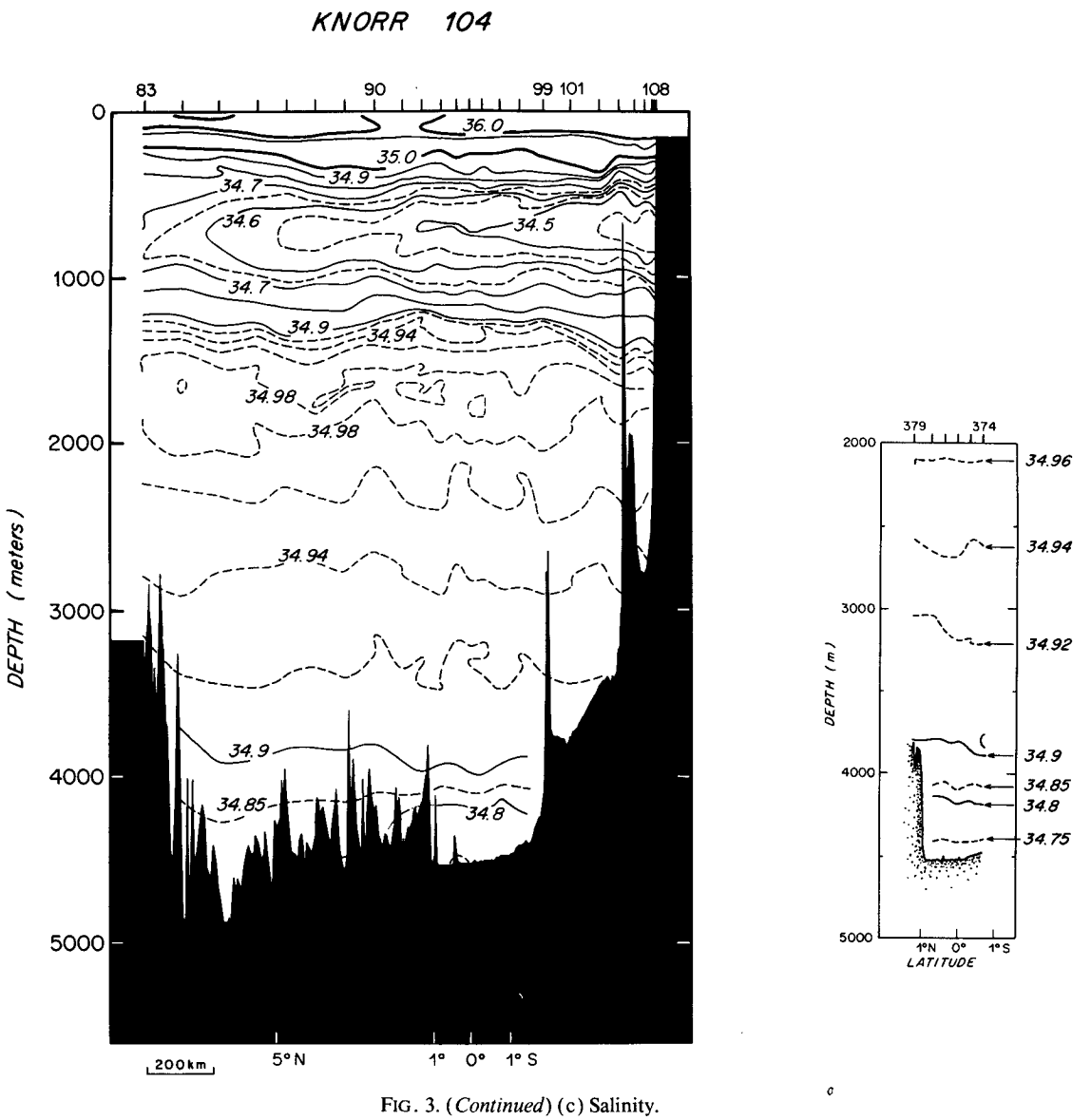

FIG. 3. (*Continued*) (c) Salinity.

It relates the velocity components to the slope of dynamic height and, for the eastward velocity component U, is, in conventional oceanographic units:

$$f[U(p) - U_r] = -10\,dD/dy, \qquad (1)$$

where the velocity is at a pressure level p, f is the Coriolis parameter, D the dynamic height relative to the pressure of a reference level, U_r is the velocity at that reference level, y is the northward coordinate, and dD/dy the northward slope of the dynamic height, with the factor of 10 required to convert the units of dynamic height to MKS units. At the equator the resulting expression for $U(p)$ is either singular, if the observed dynamic height slope is not zero, or degenerative, $0 \div 0$, if that slope is zero.

The equatorial version of the geostrophic relation for $U_{eq}(p)$, the zonal velocity at the equator, is

$$\beta[U_{eq}(p) - U_r] = -10d^2D/dy^2, \qquad (2)$$

where $\beta = df/dy$. There are at least three ways to arrive at this equation. Joyce (1988) used the same starting point that leads to the conventional expression (1) and applied a Taylor series expansion in y centered on the equator, which, retaining terms independent of y and linear in y, yields (2) and simultaneously the consistency requirement:

$$[dD/dy]_{eq} = 0. \qquad (3)$$

If this is not satisfied by the measured field, then a neglected term must be important. Joyce considers

stress as one possibility; other possibilities are time dependence and nonlinearity. Another approach (Reid 1948) differentiates (1) with respect to y, which gives (2), but implicitly assumes (3) because otherwise (1) would be an inequality. A third approach (Montgomery and Stroup 1962) asserts a y-independent zonal speed at and near the equator, which by (1) requires that the dynamic height slope is proportional to f, yielding (3). Having avoided the singularity by the assumption of uniform U, the conventional formulation (1) yields the same result as the equatorial formulation (2).

There is a philosophical point to be raised here. The methods all share (3). In our opinion, a necessary condition for the use of (2) is that the dynamic height field observed satisfy (3). If the observed field does not have the required symmetry to allow the sensible fitting of a parabola centered on the equator, we believe that the calculation should not be made. It would be possible to force fit a parabola to satisfy (3) for an arbitrary dynamic height distribution that is not parabolic in appearance, but we think that it is inadvisable. In the common applications to the equatorial undercurrent, this issue is apparent: it is normal to average many realizations of the dynamic height distribution and direct measurements of the zonal velocity before they converge to the same answer (Lukas and Firing 1984), and even then a residue of higher order effects may appear, for example, the nonhydrostatic correction described by Joyce et al. (1988). As will be seen below, the dynamic height along our first section satisfies (3), so we implement (2) and use the resulting velocity to estimate the transport of AABW westward along the equator. The dynamic height observed along our second section does not appear to satisfy (3), so the calculation is not made, and we assume some neglected term in the meridional momentum equation, like time dependence, is therefore not negligible.

The implementation of (2) at the equator is somewhat more difficult than (1) at midlatitude. A minimum of three stations is required to define the curvature of dynamic height. The five stations centered on the equator in the 1983 section are used. These (Fig. 4a) define a smooth parabola, which is characterized by applying a least squares parabolic fit to determine the curvature as a function of pressure at 20-db intervals. Application of (2) yields a profile of westward speed relative to a reference level of 4000 db where we have assumed zero speed, $U_r = 0$. This profile is interpreted as the meridional average profile over the width (167 km) of the station group defining the curvature. Multiplying by this width, and integrating downwards from the 4000-db (3940 m) reference level to the deepest common level of the stations, 4520 db (4448 m), yields a westward transport of 4.3×10^6 $m^3 s^{-1}$ of AABW colder than about 1.93°C, the average temperature at the reference level.

First used by Wright (1970), the choice of 1.9°C as a reference level has been conventionally used in studies of the abyssal circulation of the Atlantic. It marks the top of the transition layer between the AABW and NADW and we assume this to be a level of no motion. In the South Atlantic this assumption of a level of no motion is reasonable, for it yields northward flow of AABW and southward flow of NADW in the DWBC and for the net transport in basin-crossing sections. In the North Atlantic, Wright (1970) used this level of no motion to obtain northward net transports of AABW in the western basin. This is probably an incorrect choice (McCartney 1993b; Molinari et al. 1992), for at many locations along the western boundary of the low-latitude North Atlantic this choice gives northward flow of NADW in the DWBC. Instead, the level of no motion there is above the NADW, which gives southward flow of AABW in the DWBC, with the net northward flow of AABW achieved by the larger northward flow of AABW in the basin interior.

Before discussing the transport estimate in the context of other estimates of AABW flow, we note the following caveats regarding certain details.

First, our transport estimate through the equatorial channel does not incorporate bottom triangles, but instead uses only the area above the deepest common level of the five stations. By applying the speed computed at the deepest common level to the area beneath it, we could infer an additional 0.44×10^6 $m^3 s^{-1}$ of AABW transport.

Second, a zero reference level velocity is used. There is, however, evidence that the NADW above the reference level may also be moving west (McCartney 1993b). Imposing a reference level speed, U_r, would correspond to shifting the speed axis right/left by that amount in Fig. 4b. In this case, the sensitivity to a reference level speed is considerable: the effect of imposing a westward U_r of 1 cm s^{-1} is to add 0.9×10^6 $m^3 s^{-1}$ to the westward transport. Exploring this important issue further, however, is beyond the scope of this paper.

Third, this five-station group does not constitute complete coverage of the equatorial channel; in fact there is additional AABW to the north and south of this group depicted by stations 92–93 and 97–98–99 in Fig. 3a. The isotherms in each of these two station groups reverse their trend away from the core of the equatorial current, sloping downward toward each of the channel walls. This is the shear signature of eastward AABW flow. The nature of the Coriolis parameter at these latitudes and a difficult bottom triangle situation preclude us from attempting any transport estimates here. These possible eastward flows at the northern and southern edges of the equatorial channel would act to reduce the net AABW transport, thus acting in a sense to compensate for the effects described in the first two caveats.

Fourth, the representativeness of the AABW property fields over time is uncertain. The 1989 realization

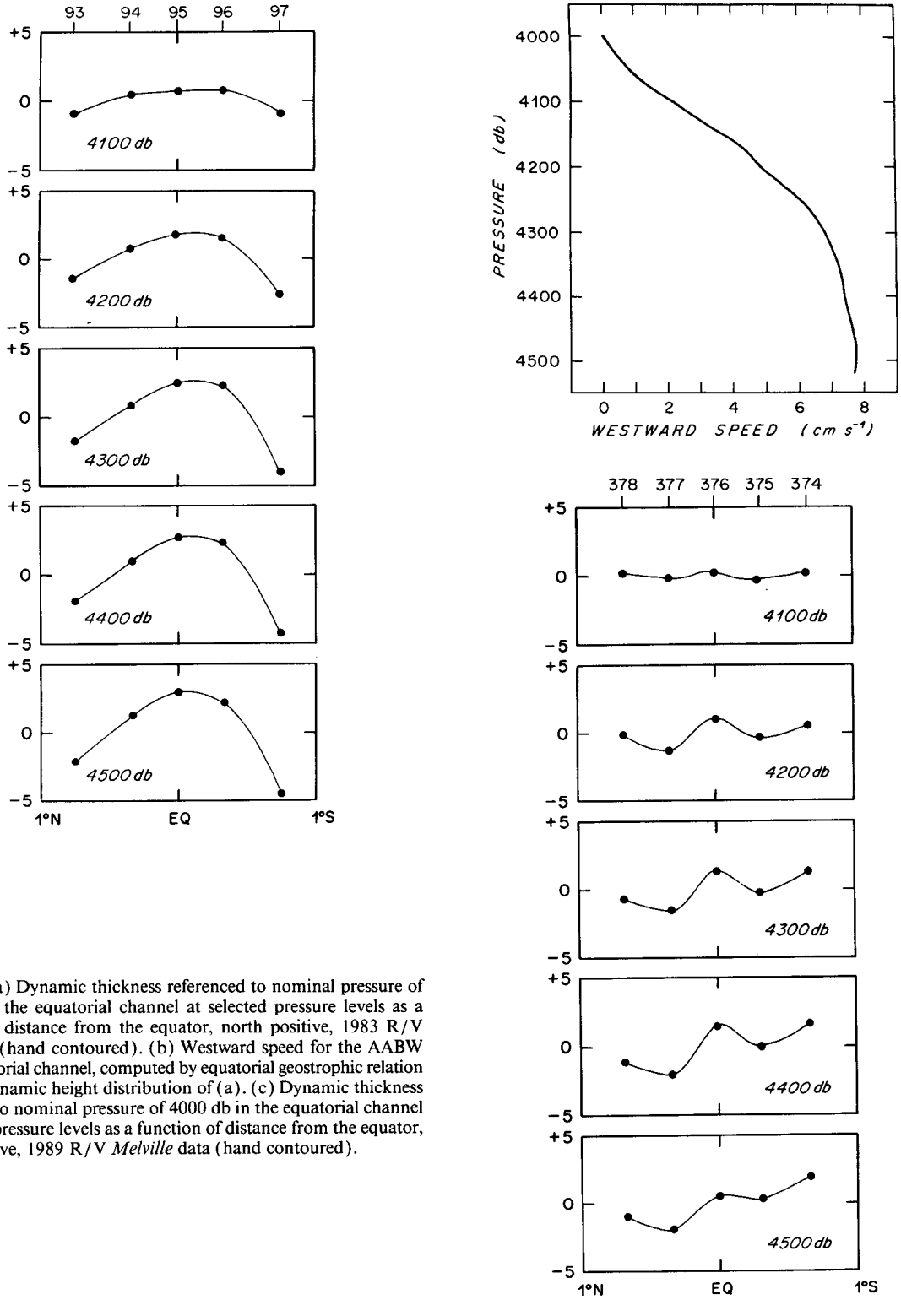

FIG. 4. (a) Dynamic thickness referenced to nominal pressure of 4000 db in the equatorial channel at selected pressure levels as a function of distance from the equator, north positive, 1983 R/V *Knorr* data (hand contoured). (b) Westward speed for the AABW in the equatorial channel, computed by equatorial geostrophic relation from the dynamic height distribution of (a). (c) Dynamic thickness referenced to nominal pressure of 4000 db in the equatorial channel at selected pressure levels as a function of distance from the equator, north positive, 1989 R/V *Melville* data (hand contoured).

of the AABW dynamic height in the equatorial channel (Fig. 4c) shows a narrower parabola defined by three stations at the equator, but with the five stations showing an overall slope at the equator, in violation of the constraints of the equatorial geostrophic formulation. Ignoring the slope, the curvature is about double that

of the first realization, and the width about half; perhaps the transport would be about the same. But lacking the robustness of the full five-station parabola, we have not made the calculation for the 1989 data.

Fifth, there remains a possibility that the north wall of the equatorial channel may have a gap deep enough to allow some flow of AABW through the wall, so that our estimate at 37°W would not represent the total transequatorial AABW flow. Our bathymetry database (averaged on a 5-minute grid) depicts a gap in the north wall between 36° and 37°W where depth exceeds 4000 m. Bathymetry recorded on each of the CTD cruises, however, places the crest above 3800 m in this supposed gap.

These caveats notwithstanding, the estimate of 4.3 $\times 10^6$ m^3 s^{-1} of transequatorial AABW transport fits rather well with other Atlantic AABW transport estimates, detailed next. In September 1992, an array of six moorings separated by 55 km was deployed across the equatorial channel near 36°W for two years, each mooring instrumented with three to seven current meters in the AABW and lower NADW. Our hope is to quantify directly the AABW transport and by also monitoring temperature validate the equatorial geostrophic relationship by comparing the meridional distributions of zonal speed and temperature.

4. Antarctic Bottom Water transport in the western trough of the Atlantic Ocean

Several difficulties complicate an attempt to construct a cohesive picture of AABW transport through the western trough from existing estimates. Differences in methodology among investigators, for example, selection of level of no motion (LNM), bottom triangle approximation, and station placement, often lead to discrepancies of the same order as the transport estimate itself. McCartney (1993a) illustrates the dependence of transport estimates in the southern Guiana Basin on the LNM showing that a variation of ±0.2°C an LNM results in a change of $\pm 0.8 \times 10^6$ m^3 s^{-1} or 20% of an estimated 4.0×10^6 m^3 s^{-1} for AABW below an LNM = 1.9°C at 4°N. Using the same LNM, Whitehead and Worthington (1982) had previously estimated only 2.0×10^6 m^3 s^{-1} for the same data. The discrepancy is caused (McCartney 1993a) equally by computational flaws in the Whitehead and Worthington original calculations and by differences in bottom triangle approximations. Another complication inhibiting intercomparison of existing transport estimates lies in the definition of AABW. Because it is an advective–diffusive system, over long distances AABW characteristics change, while the counteracting processes of vertical advection and downward diffusion cause the top of the AABW layer to be ambiguously defined. As the AABW characteristics evolve from basin to basin and between hemispheres, investigators vary on how they define and where they choose to place that boundary.

In the Brazil Basin, 1983 CTD surveys located at 23° and 11°S (Fig. 5) yield net northward AABW transports of 6.7×10^6 m^3 s^{-1} and 5.5×10^6 m^3 s^{-1}, respectively, for AABW below an LNM = 1.9°C. For purposes of comparison, Wright (1970) provides us with a treatment of sections crossing the western trough during the IGY. From sections located in the Brazil

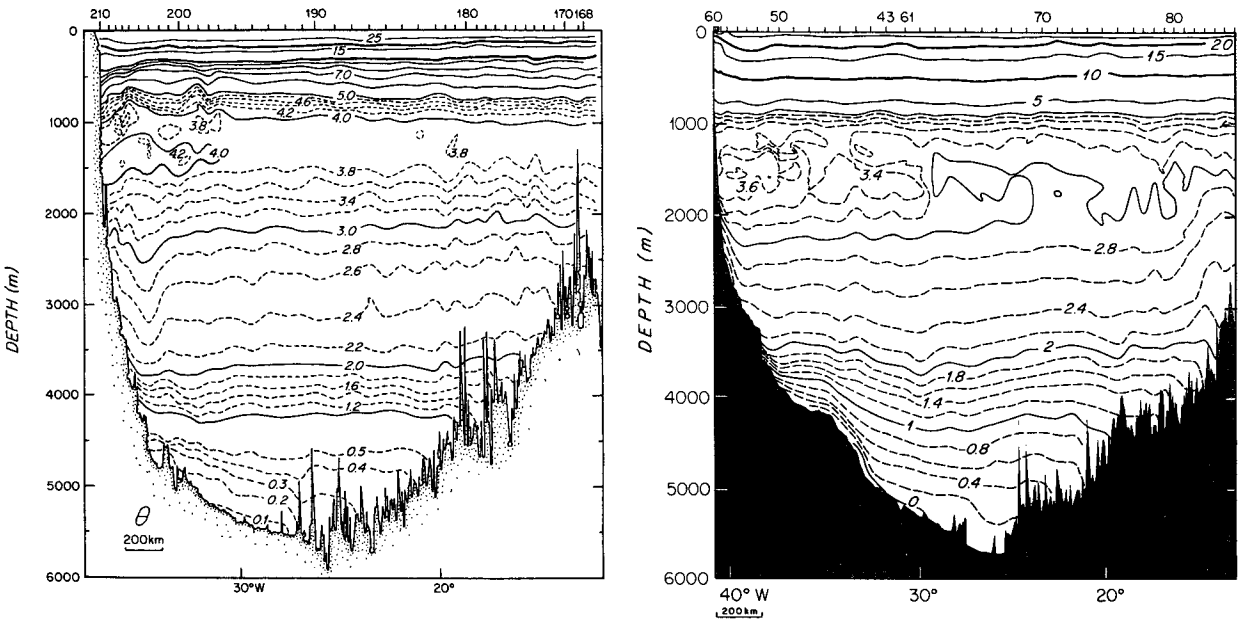

FIG. 5. Potential temperature (°C) along a zonal section made from R/V *Oceanus* (a) near 11°S (position shown on Fig. 2a) in March 1983 and (b) near 23°S (position shown on Fig. 2a) in February 1983.

Basin at 24°S, 16°S, and 8°S, he reports transports of 6.4×10^6 m^3 s^{-1}, 2.3×10^6 m^3 s^{-1}, and 2.8×10^6 m^3 s^{-1}, respectively—a somewhat troublesome scatter. Significant improvement in station resolution at the western boundary, the quality of CTD technology, or a change in intensity of the AABW system between the 1950s and 1980s may account for some of the discrepancy between the two sets of estimates. Certain other differences are noted in methodology, again concerning bottom triangle approximation and choice of LNM. Wright used the Helland-Hansen (1934) method of extrapolating dynamic height in the bottom triangle. This essentially extrapolates dynamic height horizontally from a deep station to a shallow station everywhere below a level representing the greatest common depth. We compute the shear between station pairs above the greatest common depth and extrapolate downward, weighted by the vertical density gradient. For an LNM, Wright defined the AABW/NADW interface as the sharp break in temperature and salinity gradients that he noted in station profiles from the IGY sections. He asserted that because NADW moves south and AABW moves north, this interface represents a level of no motion. It is unclear at what scale he applied this assertion, defining the LNM at the slope change for individual stations or defining the slope change in terms of a temperature for an entire section. He only noted that this reference level corresponds "roughly" to the 2.0°C isotherm and 34.89 psu isohaline and slopes from about 3400 m at 32°S to 4400 m at 16°N. Although we cannot specifically pinpoint causes for the large discrepancies between transport values, we believe our methods are valid and hope that the quality of these estimates has at least been improved.

Our estimates in the central Brazil Basin indicate transport values that average about 6×10^6 m^3 s^{-1} for AABW below an LNM of 1.9°C and decline northward. From moored current meter data and CTD surveys, Hogg et al. (1982) estimated an AABW transport of 4.1×10^6 m^3 s^{-1} entering the basin through the Vema Channel using a reference level near 2.0°C (their reference level is actually defined by a density surface $\sigma_4 = 45.91$). Speer and Zenk (1993) suggest an additional flow of 2.0×10^6 m^3 s^{-1} occurs over the continental slope west of the Vema Channel. Speer et al. (1992) estimate 0.7×10^6 m^3 s^{-1} passes northward through the Hunter Channel between the Rio Grande Rise and the Mid-Atlantic Ridge. Combining these produces an estimate of about 6.8×10^6 m^3 s^{-1}, only slightly larger than our estimate at 23°S.

The northward decline of AABW transport in the Brazil Basin suggests vertical motion of water across isotherms. The uneven nature of the decline may reflect the roughness of the transport estimates: almost no decline between the southern inflow and 23°S and a sharp decline from 23°S to 11°S. We can estimate the upwelling velocity between 23° and 11°S as 3.4×10^{-5} cm s^{-1} by dividing the difference in transports, 1.13×10^6 m^3 s^{-1}, by the area between the sections. This is virtually identical to the upwelling velocity across 4000 m estimated by Warren and Speer (1991) south of 11°S in the eastern basin; however, we agree with their comment that these speeds seem "suspiciously high." Our estimate of upwelling velocity is extremely sensitive to several factors. Had the decline in transport between 11°S and the Brazil Basin inflows near 30°S been considered, the upwelling transport would have increased to 1.4×10^6 m^3 s^{-1}, accompanied by a significant decrease in upwelling velocity to less than 2×10^{-5} cm s^{-1} due to the larger area of upwelling. Similarly, using a slightly colder reference level of 1.8°C alters the 23° and 11°S transport estimates only slightly (a few percent each) to 6.6×10^6 m^3 s^{-1} and 5.8×10^6 m^3 s^{-1} but reduces the apparent upwelling transport by 33% to 0.74×10^6 m^3 s^{-1} and the estimated upwelling velocity to 2.2×10^{-5} cm s^{-1}. Thus, the upwelling speed, found from the differences in transports between successive sections, is rather more sensitive to the transport estimate uncertainties than the individual estimates since it involves subtracting two transports of nearly equal size.

Antarctic Bottom Water exits the Brazil Basin to the north across the equator and to the east through the Romanche Fracture Zone. Our estimate of the transequatorial transport in the western basin is 4.3×10^6 m^3 s^{-1}, and the difference between this and the 11°S estimate of 5.5×10^6 m^3 s^{-1}, namely 1.2×10^6 m^3 s^{-1}, is therefore an estimate of the sum of the eastward flow through the Romanche Fracture Zone and the upwelling across the 1.9°C isotherm between 11°S and the equator. There presently exists no direct estimate of the Romanche flow. Warren and Speer have made an indirect estimate by combining their estimated southward deep western boundary current transport at 11°S in the eastern basin, 0.70×10^6 m^3 s^{-1}, with an abyssal circulation model that shows the required equatorial source (the Romanche flow) to be roughly three times that value, about 2×10^6 m^3 s^{-1}. But they note that this "is probably an overestimate because its basis also led to the suspiciously high upwelling velocities."

In the Guiana Basin, θ_B values trace the AABW as it spreads northward and delineate its passage into the eastern basin through the Vema Fracture Zone at 11°N (Fig. 1). McCartney et al. (1991) quantify the flow through the Vema Fracture Zone for water colder than 2.0°C as 2.2×10^6 m^3 s^{-1}. For comparison purposes, it is reported here that the flow recomputed for AABW colder than 1.9°C is about 1.9×10^6 m^3 s^{-1}. At 4°N, in the Ceara Abyssal Plain south of the Vema Fracture Zone, the transport is estimated at 4.0×10^6 m^3 s^{-1} (McCartney 1993a). Siphoning the estimated transport of AABW through the Vema Fracture Zone leaves slightly more than 2.1×10^6 m^3 s^{-1} to continue northward in the western basin. An energetic abyssal cyclonic

gyre (McCartney 1993b) complicates the recognition of the net northward AABW transport in the Guiana Basin, which is achieved as the differences between a northward transport in the basin interior and a southward flow of AABW in the DWBC of the basin. It appears that this net flow is on the order of 2×10^6 $m^3 s^{-1}$.

5. Discussion

We have described a zeroth-order transport scheme for the Brazil and Guiana basins, roughly defining the net AABW transport at several locations, and note a northward decline of AABW transport, which suggests upwelling into the overlying deep water. About 7×10^6 $m^3 s^{-1}$ enters the Brazil Basin from the south, of which about 4.3×10^6 $m^3 s^{-1}$ crosses the equator to continue northward in the Guiana Basin. The difference, 2.7×10^6 $m^3 s^{-1}$, is an indirect estimate of the combined upwelling and the eastward flow out of the northern Brazil Basin into the eastern basin. It is zeroth order for a number of reasons but predominately due to the nature of geostrophic calculations, equatorial or midlatitude. The unresolved bottom triangles beneath the deepest common levels of the hydrographic sections are particularly troublesome for the AABW overlying the bottom. We have used the boundary between the AABW and NADW as an LNM, a choice that seems to give consistent AABW and NADW transport directions and magnitudes in the South Atlantic. But that choice is known to be inappropriate in the Guiana Basin of the North Atlantic. Whether the equatorial geostrophic estimate is sensible and accurate will hopefully be determined by the equatorial moored array mentioned earlier, while a second array now in place in the Romanche Fracture Zone may sharpen the estimate there. Additional hydrographic sections have been made across the Brazil Basin in 1988–91, and a major study of the abyssal circulation of that basin is now under way (the Deep Basin Experiment of the World Ocean Circulation Experiment). Soon, therefore, we hope the scheme we describe here will be refined and replaced with a first-order scheme where, for example, a net vertical flow upward from the AABW to the NADW can be recognized and quantified as a difference between inflow and outflow transports or as the difference in net transport between two basin-crossing sections.

In our present zeroth-order budget the northward decline in transport is suggestive of the effect of upwelling across the 1.9°C isotherm. The transport estimates are not, however, adequate to allow the subtraction of successive transport estimates to determine a distribution of upwelling, and the lack of a direct transport estimate at the Romanche Fracture Zone further clouds the interpretation of the transport residues. Upwelling is intimately tied to warming of the AABW along the flow: if there is upwelling, then there must be downward diffusion of heat to maintain a steady state (since there is no evidence in historical data for basin-scale evolution of the AABW in the Brazil Basin). Figure 6 shows distribution of the total transport of AABW in temperature classes for several of the locations. While the mass balances are inadequate to allow a detailed interpretation of the fluxes in each layer and the upwelling between layers, these distributions do show the warming of the dominant transport contributions moving from 32°S[2] through

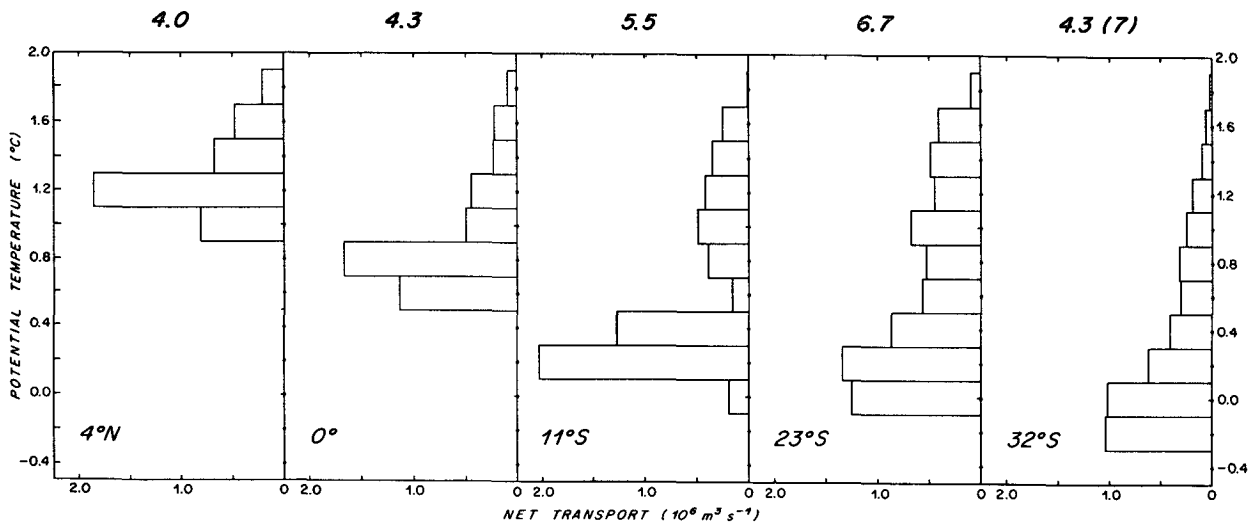

FIG. 6. Net AABW transport in layers defined by isotherms at the indicated primary geographic locations discussed in the text. These illustrate the warming of the dominant transport mode, as the colder levels of AABW upwell into the warmer levels. The large numbers at the top of each graph are the net AABW transports below 1.9°C for each location in 10^6 $m^3 s^{-1}$ except at 32°S where the graph represents the Vema Channel flow only, about 60% of the total flow of 7×10^6 $m^3 s^{-1}$ (see text).

the Brazil Basin across the equator to 4°N in the Guiana Basin. The figure mirrors the θ_B chart of Fig. 1 by showing a rather more gradual increase of the transport mode temperature within the Brazil Basin compared to the transequatorial warming of the transport mode in passage over the equatorial sill. Thus, our zeroth-order budget does demand a significant upwelling of the colder AABW classes into warmer ones, and, for a steady-state heat balance, a downward diffusion of heat. This is consistent with the classical image from Wüst (1933) of the progressive warming of the AABW following its flow from the southern source through the western basin of the North Atlantic.

Acknowledgments. The authors thank Mindy Hall and Terry Joyce for discussions of transequatorial transport issues, Bill Schmitz for stimulating this detailed examination of the data, and Mary Woodgate-Jones for her assistance with the equatorial geostrophic calculations. Bruce Warren is thanked for making available to the authors the 11°S section data. Theresa Turner is thanked for her careful work in preparing the analysis products reported on here and Veta Green and Barbara Gaffron for the preparation of the manuscript. This work was supported by the National Science Foundation under Grants OCE86-14486 and OCE91-05834 and the Atlantic Climate Change Program of the National Oceanic and Atmospheric Administration under Grant NA16RC0528-01.

REFERENCES

Hayes, S. P., 1982: A comparison of measured and geostrophic velocities in the Equatorial Undercurrent. *J. Mar. Res.*, **40**(Suppl.), 219–229.

Helland-Hansen, B. J., 1934: The Sognefjord section. *James Johnstone Memorial Volume,* Liverpool University Press, 257–274.

Hogg, N., P. Biscaye, W. Gardner, and W. J. Schmitz, Jr., 1982: On the transport and modification of Antarctic Bottom Water in the Vema Channel. *J. Mar. Res.*, **40,** 231–263.

Joyce, T. M., 1988: Wind-driven cross-equatorial flow in the Pacific Ocean. *J. Phys. Oceanogr.*, **18,** 19–24.

——, R. Lukas, and E. Firing, 1988: On the hydrostatic balance and equatorial geostrophy. *Deep-Sea Res.*, **35,** 1255–1257.

Lukas, R., and E. Firing, 1984: The geostrophic balance of the Pacific Equatorial Undercurrent. *Deep-Sea Res.*, **31,** 61–66.

Mantyla, A. W., and J. L. Reid, 1983: Abyssal characteristics of the World Ocean waters. *Deep-Sea Res.*, **30,** 805–833.

McCartney, M. S., 1992: Recirculating components to the deep boundary current of the northern North Atlantic. *Progress in Oceanography,* Vol 29(4), Pergamon Press, 293–393.

——, 1993a: The transport of Antarctic Bottom Water at 4°N in the western basin of the North Atlantic Ocean. *J. Geophys. Res.,* in press.

——, 1993b: The crossing of the equator by the deep western boundary current in the western Atlantic Ocean. *J. Phys. Oceanogr.,* in press.

——, S. L. Bennett, and M. E. Woodgate-Jones, 1991: Eastward flow through the Mid-Atlantic Ridge at 11°N and its influence on the abyss of the eastern basin. *J. Phys. Oceanogr.*, **21,** 1089–1121.

Molinari, R. L., R. A. Fine, and E. Johns, 1992: The deep western boundary current in the tropical North Atlantic Ocean. *Deep-Sea Res.*, **39,** 1967–1984.

Montgomery, R. B., and E. D. Stroup, 1962: Equatorial waters and currents at 150°W in July–August 1952. *The Johns Hopkins Oceanographic Studies,* **1,** 68 pp.

Moum, J. N., T. K. Chereskin, M. M. Park, and L. A. Regier, 1987: Monitoring geostrophic currents at the equator. *Deep-Sea Res.*, **34**(7), 1149–1161.

National Geophysical Data Center, 1988: Digital relief of the surface of the earth. Data Announcement 88-MGG-02, NOAA, Boulder, CO.

Ponte, R. M., J. Luyten, and P. L. Richardson, 1990: Equatorial deep jets in the Atlantic Ocean. *Deep-Sea Res.*, **37**(4), 711–713.

Reid, R. O., 1948: The equatorial currents of the eastern South Pacific as maintained by the stress of the wind. *J. Mar. Res.*, **7,** 74–99.

Speer, K. G., and W. Zenk, 1993: The flow of Antarctic Bottom Water across the Rio Grande Rise. *J. Phys. Oceanogr.,* in press.

——, W. Zenk, G. Siedler, J. Pätzold, and C. Heidland, 1992: First resolution of flow through the Hunter Channel in the South Atlantic. *Earth Plan. Sci. Lett.*, **113,** 287–292.

Warren, B. A., and K. G. Speer, 1991: Deep circulation in the eastern South Atlantic Ocean. *Deep-Sea Res.*, **38**(Suppl. 1), S281–S322.

Whitehead, J. A., and L. V. Worthington, 1982: The flux and mixing rates of Antarctic Bottom Water within the North Atlantic. *J. Geophys. Res.*, **87,** 7903–7924.

Whitworth, T., III, W. D. Nowlin, Jr., R. D. Pillsbury, M. I. Moore, and R. F. Weiss, 1991: Observations of the Antarctic Circumpolar Current and Deep Boundary Current in the Southwest Atlantic. *J. Geophys. Res.*, **96**(C8), 15 105–15 118.

Wright, W. R., 1970: Northward transport of Antarctic Bottom Water in the western Atlantic Ocean. *Deep-Sea Res.*, **17,** 367–371.

Wüst, G., 1933: Schichtung und Zirkulation des Atlantischen Ozeans. Das Bodenwasser und die Gliederung der Atlantischen Tiefsee. *Wissenschaftliche Ergebnisse der Deutschen Atlantischen Expedition auf dem Forschungs- und Vermessungsschiff "Meteor" 1925–1927,* **6,** 1st Part, 1, 106 pp. [1967: *Bottom Water and the Distribution of the Deep Water of the Atlantic,* M. Slessers, Transl., B. E. Olson, Ed., U.S. Naval Oceanographic Office, 145 pp.]

[2] At 32°S, the various data used by Speer et al. (1992) and Speer and Zenk are not available in a form to do this calculation simply. In the plot, one of the ten sections used by Hogg et al. (1982) to obtain their geostrophic estimate of the average transport, 4.15 $\times 10^6$ m^3 s^{-1}, through the Vema Channel is used. The one selected (*Atlantis II* cruise 107 leg 2, section 5 of their study) gives a transport (their Table 2) closest to this mean, 4.34 $\times 10^6$ m^3 s^{-1}. Applying our level of no motion of 1.9°C recovers almost the identical transport, 4.33 $\times 10^6$ m^3 s^{-1}.